HiFSA Fingerprinting Applied to Isomers with Near-Identical NMR Spectra: The Silybin/Isosilybin Case

By: José Napolitano, David C. Lankin, Tyler N. Graf, J. Brent Friesn, Shao-Nong Chen, James B. McAlpine, Nicholas H. Oberlies, Guido F. Pauli

Napolitano, J.G.; Lankin, D.C.; Graf, T.N.; Friesen, J.B.; Chen, S.-N.; McAlpine, J.B.; Oberlies, N.H.; Pauli, G.F. HiFSA Fingerprinting Applied to Isomers with near-Identical NMR Spectra: The Silybin/Isosilybin Case. *The Journal of Organic Chemistry*, *2013*, *78*, 2827-2839.

Abstract:

This study demonstrates how regio- and diastereo-isomers with near-identical NMR spectra can be distinguished and unambiguously assigned using quantum mechanical driven 1H iterative Full Spin Analysis (HiFSA). The method is illustrated with four natural products, the flavonolignans silybin A, silybin B, isosilybin A, and isosilybin B, which exhibit extremely similar coupling patterns and chemical shift differences well below the commonly reported level of accuracy of 0.01 ppm. The HiFSA approach generated highly reproducible 1H NMR fingerprints that enable distinction of all four isomers at 1H frequencies from 300 to 900 MHz. Furthermore, it is demonstrated that the underlying numeric 1H NMR profiles, combined with iterative computational analysis, allow parallel quantification of all four isomers, even in difficult to characterize reference materials and mixtures. The results shed new light on the historical challenges to the qualitative and quantitative analysis of these therapeutically relevant flavonolignans and open new opportunities to explore hidden diversity in the chemical space of organic molecules.

Graphical Abstract:

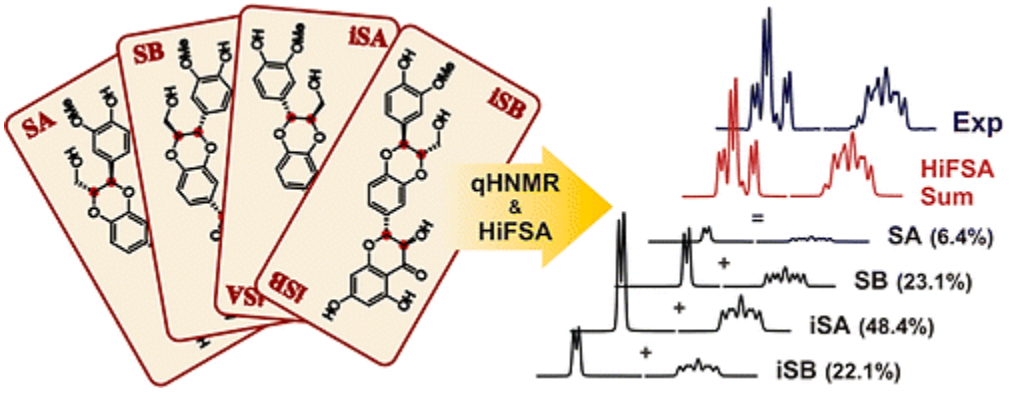

Keywords: Organic chemistry | Milk thistle | flavonolignans | silybin | HiFSA | NMR profiles

Article:

Introduction

The occurrence of isomers is a key source of structural diversity in organic, natural product, and biological chemistry. Isomers often exhibit different chemical, physical, and/or biological properties and, with the exception of enantiomers, are also expected to exhibit different nuclear magnetic resonance (NMR) spectra.[(1)] These general assumptions are based on both structural and spatial considerations. Given their diverse atomic arrangements, constitutional isomers (i.e., regioisomers) frequently exhibit substantial differences in chemical shifts (δ) due to differences in the nuclei's local electronic and, therefore, magnetic environments.[(2-4)] In addition, different spin-coupled systems commonly exhibit different signal splitting patterns. In the case of diastereomers, changes in relative configurations give rise to substituent-induced chemical shift effects.[(3, 5)] Moreover, variations in the relative position of substituents frequently produce changes in the magnitude of spin-spin coupling constants (*J*).[(6)] These observations, combined with the connectivity information obtained from multidimensional NMR experiments, support the prevailing hypothesis that regioisomers and diastereomers have distinctive NMR profiles.

However, isomeric compounds with very similar *J*-coupling patterns may exhibit near-identical ^{1}H NMR spectra. In such cases, our ability to distinguish their 1D NMR profiles rests exclusively on the recognition of chemical shift differences (Δδ). In fact, as δ values are influenced by several variables, including solvent, analyte concentration, salt content, temperature, and pH, these differences may be very small. In addition, the accuracy of chemical shift measurements is limited by the digital resolution of the acquired spectrum. Reflecting these factors, δ values are commonly reported to only 0.01 ppm accuracy, and hence, the differences between individual ^{1}H NMR resonances must exceed 0.01 ppm in order for the isomers to be recognized as such. When the Δδ values fall below this threshold, identification of individual compounds by NMR can be challenging or impossible.

Nature Produces Hidden Isomers

The present study describes the complete ^{1}H and ^{13}C NMR spectral analysis of a set of closely related regio- and diastereo-isomers that, despite having spatially distinct 3D structures, exemplify the analytical challenge of distinguishing molecules with near-identical ^{1}H NMR spectra. The compounds selected for this study are a group of natural products obtained from the fruits of *Silybum marianum* (L.) Gaertn. (milk thistle), commonly referred to as silybins and isosilybins (see Chart 1 and the Supporting Information for nomenclature and numbering). The major constituents are the isomers silybin A (**1**), silybin B (**2**), isosilybin A (**3**), and isosilybin B (**4**), which exhibit only very minor, subtle differences in their ^{1}H NMR profiles. As a result, isomers with near-identical NMR spectra can fail to be distinguished. This lack of definition may become important for a better understanding of why, for more than five decades, silybins and

isosilybins have presented a wealth of challenging interdisciplinary research problems. Since the onset of their detailed chemical investigation in 1960, more than 300 chemical and biological reports have appeared for compounds **1**–**4**. Between 1960 and the mid-1980s, invaluable contributions to the understanding of the chemistry of silybins and isosilybins came from the research groups and collaborators of Hänsel[7-14] and Wagner.[15-23] Subsequently, the refinement of analytical methods led to the separation of the silybin diastereoisomers and the 1:1 mixture of the silybin diastereoisomers, silibinin,[24-26] as well as the purification of **1** and **2**.[27, 28] In 2003, Kim et al. reported a comprehensive analysis of seven major *Silybum* constituents,[29, 30] and their stereochemical assignments were subsequently confirmed by Lee and Liu via single-crystal X-ray crystallography of **3**.[31, 32]

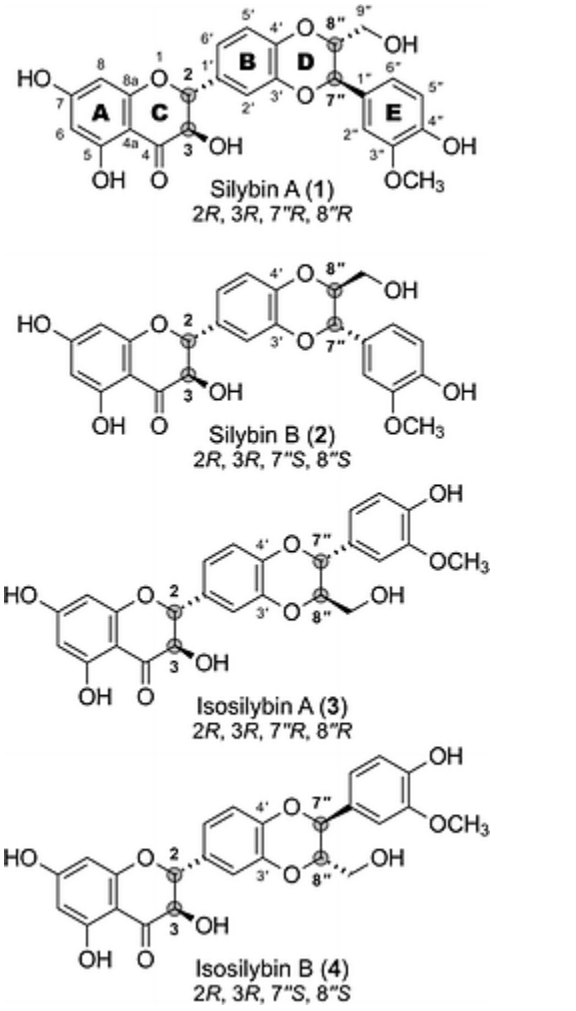

Chart 1. Structures and Numbering of the Diastereomeric Pairs of Regioisomers Silybins A and B (1 and 2) and Isosilybins A and B (3 and 4)

The Bioanalytical Challenges of *Silybum* Flavonolignans

Milk thistle preparations have been used for more than 2000 years to treat a variety of ailments, particularly liver conditions.[33-35] The beneficial properties of *Silybum* are ascribed to silymarin, a mixture of (at least) seven flavonolignans and one flavonoid that amount to 65–85% w/w of milk thistle extracts used in clinical research as well as in dietary supplements.[24] Numerous studies have shown the efficacy of silymarin as a hepatoprotective and cancer chemopreventive agent,[36-38] while also calling attention to the fact that individual silymarin constituents exhibit significantly different biological properties.[39-42] Therefore, a precise identification and quantification of specific silymarin components represents a crucial step in the investigation of structure-activity relationships of these bioactive agents, as well as the development of natural health products.

Various bioanalytical methods have been developed for the determination of *Silybum*flavonolignans.[43-50] Interestingly, they are all "separation/detection" methods in which the analytes are subjected to chromatography prior to detection by high-sensitivity techniques such as UV–vis spectrophotometry or mass spectrometry (MS). However, important limitations remain where this approach has been applied to the analysis of *Silybum* constituents. First, the separation of individual compounds from the complex mixture of regioisomers and diastereomers remains a challenging task. Second, because LC-hyphenated detection requires the establishment of response factors that depend on the specific chemical properties of each analyte, *identical* reference standards must be available for identification and calibration purposes. As the *Silybum* flavonolignans are difficult to obtain as fully characterized pure compounds, the development of a non-targeted approach by quantitative ^{1}H NMR (qHNMR) represents an attractive alternative to conventional chromatographic analysis. Given the nearly universal applicability to organic molecules and the direct proportionality between its analytical response and molar concentrations, qHNMR[51-53] is now an established technique for the examination of both reference materials and complex mixtures, and is widely applied in the chemical and pharmaceutical industry as well as organic chemistry, natural product, and metabolomic research.[54, 55] Besides quantification, qHNMR provides valuable structural information, requires only simple sample preparation and reasonably short measuring times, especially with contemporary NMR instrumentation. While the sensitivity gap between MS and NMR still remains substantial, spectral overlap represents the greatest challenge and limitation in 1D qHNMR for molecules like the *Silybum* flavonolignans. Consequently, in order to enable the NMR analysis of silybins and isosilybins, the characteristic resonances of each individual isomer must first be precisely and unambiguously identified.

Dissecting Isomeric Complexity by NMR

The *Silybum* flavonolignans are an illustrative example of natural chemical diversity that remained undefined for decades until analytical and/or synthetic methodology revealed its true complexity. It has been proposed that **1**–**4** are formed in a non-regioselective, non-stereoselective process that involves the oxidation of taxifolin and coniferyl alcohol to their corresponding phenoxy and quinone methide radicals, followed by an *O*-8″ coupling and a thermodynamically

controlled, nucleophilic attack of the remaining hydroxyl group in the B-ring, located at either C-3′ or C-4′, to position C-7″.[56-58] Interestingly, Lee and Liu, when carrying out a detailed NMR analysis of **1**–**4** at 300 MHz, recognized the spectroscopic similarities between **1** and **2**, as "evidenced by less than 0.01 ppm differences of the ^{1}H NMR chemical shifts between these two isomers".[32] These authors also emphasized that "these diastereoisomers have very similar ^{1}H and ^{13}C NMR spectra and have no characteristic signals for facile identification of individual isomers".[32]

The present study demonstrates that this distinction is in fact feasible: small chemical shift differences between compounds **1**–**4** are not only characteristic and sufficient to distinguish the four isomers, but even enable quantitative analysis in mixtures. The experimental approach involved a thorough interpretation of their ^{1}H NMR spectra in DMSO-d_6, obtained by high- and ultrahigh-field NMR at 600 and 900 MHz, followed by ^{1}H iterative Full Spin Analysis (HiFSA).[59, 60] This led to a comprehensive definition of spectral parameters [all chemical shifts (δ_H), scalar coupling constants ($^{n}J_{H,H}$), and effective linewidths ($\Delta\nu_{1/2}$)]. These encode the overall location, multiplicity, and shape of the proton resonances. The analysis of these quantum mechanical driven, reproducible ^{1}H NMR *fingerprints*, together with their distinctive ^{13}C NMR signal patterns, enables a precise determination of small, yet highly significant, differences in the NMR profiles of **1**–**4**. These differences can be further exploited by qHNMR analysis, which is demonstrated for mixtures of these compounds.

It is important to note that close NMR resemblance between isomeric compounds is not an exclusive property of the *Silybum* flavonolignans. Several examples of isomers with near-identical NMR profiles have been reported as part of natural product and synthetic organic chemistry studies (Chart 2). Two compounds closely related to **1**–**4**, the regioisomers hydnocarpin[61] and hydnocarpin-D,[62] also have near-identical ^{1}H NMR spectra. Given the difficulties of separating these two components by HPLC, Guz and Stermitz calculated the hydnocarpin/hydnocarpin-D ratio in crude synthetic fractions using the characteristic ^{1}H resonances with the greatest $\Delta\delta_H$ value (0.08 ppm).[62] The authors also indicated that "it is debatable if either the ^{1}H or ^{13}C NMR spectra alone would differentiate the two compounds unless both were available".[62]

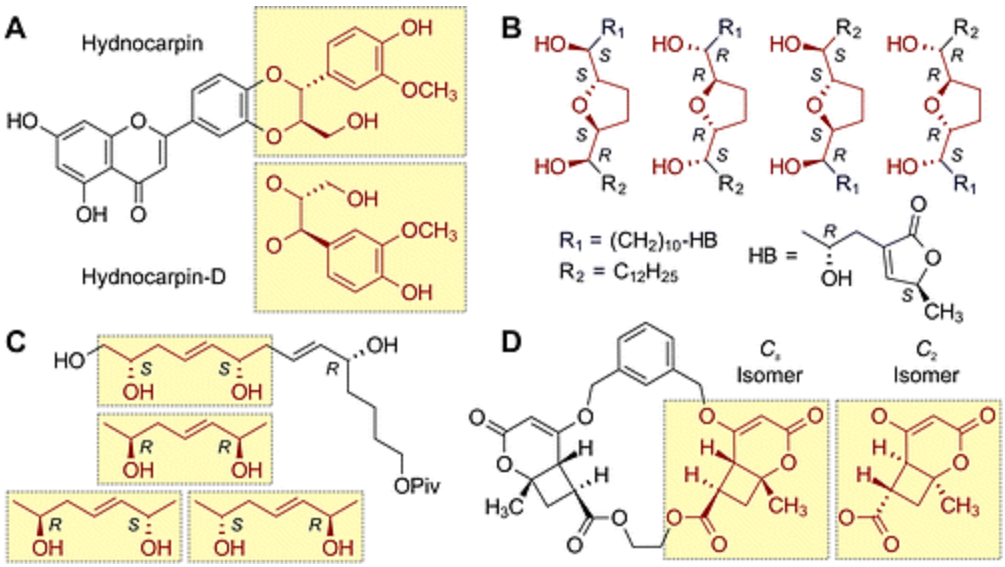

Chart 2. Additional Examples of Isomeric Organic Molecules with Near-Identical NMR Spectra: (A) Hydnocarpin/Hydnocarpin D Pair; (B) Murisolin Isomers, Exemplified with Group 1; (C) Four Diastereomers of the C-1/C-10 Fragment of Amphidinol 3; (D) Two Macrocyclic Dioxatetralactones with C_s and C_2 Symmetry, Respectively

Further prominent examples of isomers with near-identical NMR profiles exist. These include the contiguous polyols described by Kishi and colleagues, who developed ^{1}H and ^{13}C NMR databases to enable isomeric distinction. Their databases rely on the analysis of characteristic Δδ profiles to discern alternative diastereomeric configurations.(63) A fascinating example of the investigation of complex stereochemical space was carried out by Curran et al., who synthesized an extensive library of possible murisolin isomers to determine the absolute configuration of three structurally related natural products.(64) The authors observed that none of the 28 diastereomers had a unique ^{1}H or ^{13}C spectrum. In fact, considering local symmetry elements and the negligible effect of remote stereocenters, the isomeric compounds were categorized into six groups, each group with a distinctive NMR profile. Interestingly, all of the isomers within each group exhibited "substantially identical" NMR spectra, with maximum $\Delta\delta_H$ and $\Delta\delta_C$ values of 0.01 and 0.1 ppm, respectively.(64) During the synthesis of the C-1/C-10 fragment of amphidinol 3, Oishi et al. obtained four diastereomers with near-identical ^{1}H NMR spectra.(65) Still, the examination of small differences in their ^{13}C chemical shifts, with some $\Delta\delta_C$ values of less than 0.1 ppm, led to the revision of the proposed structure. Miyauchi et al. described the one-pot synthesis of two macrocyclic [2 + 2] cycloadducts with very similar ^{1}H NMR spectra. Although the two isomeric dioxatetralactones belong to different symmetry point groups, C_2 and C_s, the greatest $\Delta\delta_H$ value was only 0.07 ppm.(66) Recently, Zhang et al. synthesized four possible isomers of the C-21/C-40 fragment of tetrafibricin. These diastereoisomers also exhibit near-identical ^{1}H NMR profiles. However, "small but reliable" differences in their ^{13}C NMR spectra ($\Delta\delta_C$ values between 0.04 and 0.23 ppm) were used to differentiate the four isomers.(67) These

examples highlight the importance of small chemical shift differences in the recognition of closely related isomeric compounds.

Results and Discussion

In order to demonstrate that NMR analysis can distinguish closely related isomers, the workflow of the present study consisted of the following four main steps: (i) the isolation of the individual isomers, **1**–**4**, from their natural source and with high purity; (ii) the unambiguous assignment of all ^{1}H and ^{13}C resonances of each isomer; (iii) the generation and comparison of their ^{1}H NMR fingerprints by ^{1}H iterative Full Spin Analysis (HiFSA); and (iv) the application of these fingerprints for the qHNMR analysis of complex mixtures of the isomers.

Isolation of Silybins A and B and Isosilybins A and B

Compounds **1**–**4** were isolated using the methodology developed and optimized previously.[68] All samples were >99% w/w pure, as measured by ultra-performance liquid chromatography (UPLC) under two separate conditions (see the Supporting Information). The absolute configuration of each of the four flavonolignans was unequivocally established by electronic circular dichroism (ECD)[29] and very recently corroborated with the X-ray crystallographic analysis of the 7-*O*-*p*-bromobenzoyl derivative of **3**.[69] The purified samples were assessed for composition by qHNMR using the absolute method[53, 70, 71] and DMSO-d_6 as the solvent. The calibrated, residual protonated solvent resonance (DMSO-d_5; 2.500 ppm relative to TMS) was used as internal calibrant.[72, 73] It shall be noted that, as the amount of DMSO-d_5 in the deuterated solvent varies from lot to lot, it is necessary to carry out the calibration process for every new solvent batch, which, of course, may be used for several different qHNMR experiments. Moreover, the use of DMSO-d_6 guarantees highly consistent δ_H values over a large range of concentrations. This analysis confirmed that the separation scheme yielded high-purity isolates (>97.5% w/w by qHNMR). Only traces of organic solvents (commonly methanol) and other flavonolignans were detected as impurities (see the Supporting Information).

Assignment of ^{1}H and ^{13}C Resonances

One important prerequisite to establish ^{1}H NMR fingerprints that enable the distinction of the closely related isomers **1**–**4** is a full assignment of all of their ^{1}H and ^{13}C NMR resonances. Considering the close similarities between the NMR spectra of **1**–**4** (Figures 1 and 2), this section describes a general procedure for the unambiguous identification of individual ^{1}H and^{13}C resonances of silybins and isosilybins. The NMR assignments in DMSO-d_6 were established by a thorough analysis of 1D spectra (^{1}H and ^{13}C-DEPTQ)[74] and 2D experiments (^{1}H,^{1}H-COSY,^{1}H,^{13}C-HSQC, and ^{1}H,^{13}C-HMBC). Examination of the 1D ^{1}H NMR and 2D COSY experiments enabled the identification of five distinctive spin systems: (**I**) H-2/H-3; (**II**) H-6/H-8; (**III**) H-2′/H-6′; (**IV**) H-2″/H-6″; and (**V**) H-7″/H_2-9″. The good signal dispersion in the aliphatic region facilitated the analysis of spin systems **I** and **V** (3-spin ABC and 5-spin ABCDE-type systems, respectively). As a result, the ^{1}H resonances belonging to H-2, H-3, OH-3, H-7″,

H-8″, H-9″$_a$, H-9″$_b$, and OH-9″ were readily determined, and the corresponding ^{13}C assignments were subsequently obtained via HSQC and DEPTQ experiments. The unambiguous assignment of the*m*-coupled protons H-6 and H-8 in spin system **II** was accomplished by examination of HMBC experiments, where a diagnostic correlation between H-6 and C-5 was observed. The correlation between the exchangeable proton OH-5 and C-6 is also suitable for distinguishing the two aromatic protons in the A-ring.

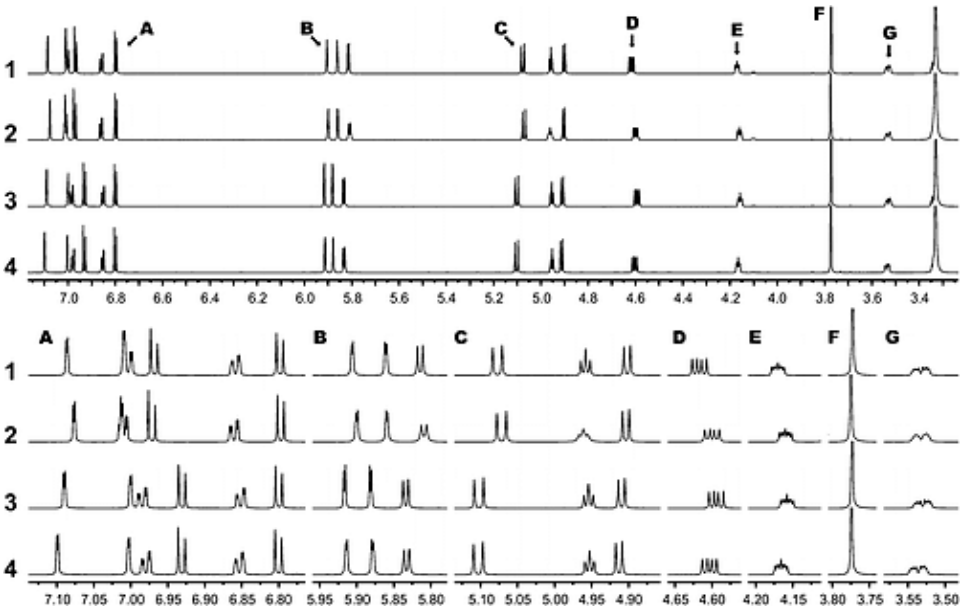

Figure 1. Stacked plots showing the similarities between the 1D ^{1}H NMR spectra of silybin A (**1**), silybin B (**2**), isosilybin A (**3**), and isosilybin B (**4**) (DMSO-d_6, 900 MHz, 298 K). Labels A–G indicate the positions of extended regions displayed in the lower panel, where small differences in ^{1}H chemical shifts between the four closely related compounds are shown.

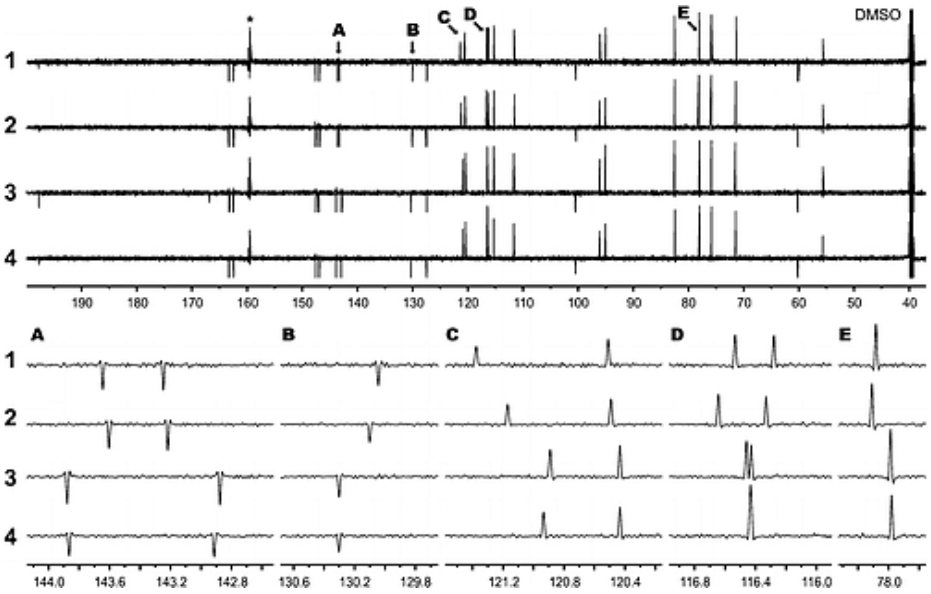

Figure 2. Stacked plots showing the similarities between the 1D ^{13}C-DEPTQ spectra of silybin A (**1**), silybin B (**2**), isosilybin A (**3**), and isosilybin B (**4**) (DMSO-d_6, 225 MHz, 298 K). Primary and tertiary carbons (CH, CH_3) are positive signals, quaternary and secondary carbons (C, CH_2) are negative signals. The artifact (*) and the DMSO signal are symmetric with respect to the center of the spectrum (i.e., transmitter offset). Labels A–E indicate the positions of extended regions shown in the lower panel, where small differences in ^{13}C chemical shifts between the four isomers are highlighted.

The ^{1}H assignments of the AMX-type systems **III** and **IV** were established by COSY to circumvent the signal overlap problem, and the ^{13}C assignments were obtained by inspection of HSQC and HMBC experiments. Therefore, the downfield, oxygen-bearing aromatic carbons in the coniferyl E-ring, C-3″ and C-4″ (δ_C ~147 ppm), can be differentiated from their counterparts in the flavonoid B-ring, C-3′ and C-4′ (δ_C ~143 ppm). However, the resolution of conventional HMBC experiments, with a 220 ppm window in the ^{13}C dimension, is typically insufficient to discriminate resonances within a narrow 2.0 ppm range, as is the case of C-3′ and C-4′. The assignment of these oxygenated carbons represents a substantial problem because, in order to distinguish the silybin and isosilybin regioisomers, it is necessary to unequivocally establish the two ether bridges that connect C-3′ and C-4′ to C-7″ and C-8″.

To obtain the critical assignments of C-3′, C-4′, C-3″, and C-4″, semiselective 2D ^{1}H,^{13}C-HMBC experiments were acquired using a 20 ppm ^{13}C window centered at 145 ppm.[(75)] These experiments not only facilitated the assignment of the carbons mentioned above, but also enabled the identification of the key connectivities between spin systems **III** and **V**: in silybin A and silybin B (**1** and **2**), correlations between H-7″ and C-3′ were observed; in contrast, isosilybin A and isosilybin B (**3** and **4**) exhibited correlations between H-7″ and C-4′ (Figure 3). In addition, the position of the methoxy group in the E-ring was confirmed via the HMBC correlation between the methoxy protons and carbon C-3″. Further analysis of the HMBC data enabled the identification of the linkages between the remaining spin systems. The correlations between the quaternary carbon C-1″ and the neighboring protons H-2″, H-6″, and H-7″ allowed the connection of spin systems **IV** and **V**. The connectivities of C-1′ to protons H-2, H-3, H-2′, and H-6′ established links between spin systems **I** and **III**. Finally, the straightforward assignment of position C-4, the only carbonyl carbon, as well as the quaternary carbons C-4a and C-8a, was essential to connect spin systems **I** and **II**.

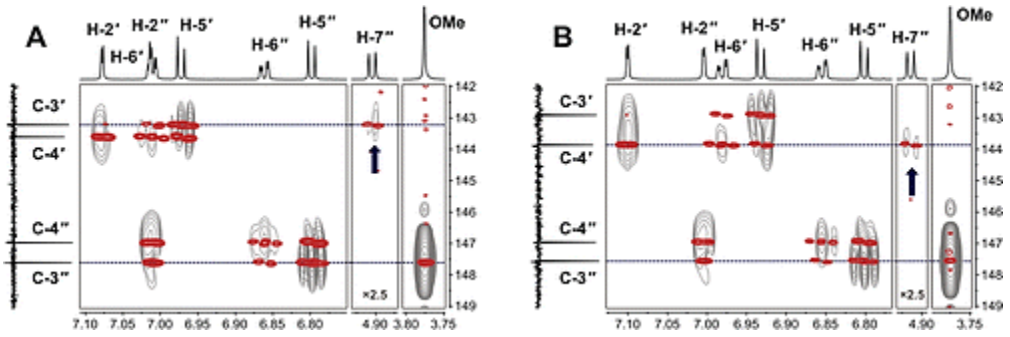

Figure 3. Identification of key HMBC connectivities to distinguish between the regioisomers silybin B (**A**) and isosilybin B (**B)** required the acquisition of 2D semiselective HMBC experiments (DMSO-d_6, 600 MHz, 298 K). In both cases, conventional HMBC experiments acquired with a 220 ppm window in the ^{13}C dimension (gray) are compared to ^{13}C resolution-enhanced, semiselective HMBC experiments acquired with a 20 ppm ^{13}C window centered at 145 ppm (red).

Generation of ^{1}H NMR Fingerprints

A complete ^{1}H NMR spectral analysis of compounds **1**–**4** was carried out by HiFSA[(59)] with PERCH NMR software.[(76, 77)] The HiFSA approach has been recently established and applied to the examination of terpene lactones and flavonoids in *Ginkgo biloba*, producing highly detailed ^{1}H NMR profiles based on field-independent parameters.(59) Scheme 1 summarizes the generation of ^{1}H NMR fingerprints in a simplified four-step protocol. In step 1, the experimental (observed)^{1}H NMR spectra, used as reference during the whole process, were imported into PERCH and subjected to basic processing and postprocessing operations, such as baseline correction, peak picking, and integration. Next, 3D molecular structures of **1**–**4** were built using the crystal structure of **3** (CCDC No. 217777)[(32)] as a template. The molecular structures were refined by geometry optimization and subjected to conformational analysis using Metropolis Monte Carlo and Molecular Dynamics simulations. The conformational space was subsequently sampled, and basic NMR parameters such as δ_H, $^nJ_{H,H}$, and $\Delta\nu_{1/2}$ were predicted using the semiempirical model in PERCH. This calculation of spectral parameters based on 3D molecular models creates a link between the chemical structure of the analyzed compounds and their individual ^{1}H NMR assignments. It also generates parameter sets with comprehensive *J* coupling patterns that are suitable starting points for the iteration process. The predicted NMR parameters were then used to simulate the ^{1}H NMR spectrum by quantum mechanics based calculations. Subsequently, the predicted δ_H values were manually adjusted in step 2, using the preliminary chemical shifts obtained during 1D/2D NMR analysis. This manual δ_H correction provided a good starting point for the subsequent optimization, using Quantum-Mechanical Total Line Shape (QMTLS) iterators,[(78)] in steps 3 and 4. This procedure led to a systematic refinement of all the calculated NMR parameters until the simulation outcome was in excellent agreement with the experimental data. When compared to the observed ^{1}H NMR spectra, all of the calculated spectra showed root-mean-square deviation (rmsd) values of less than 0.1%.

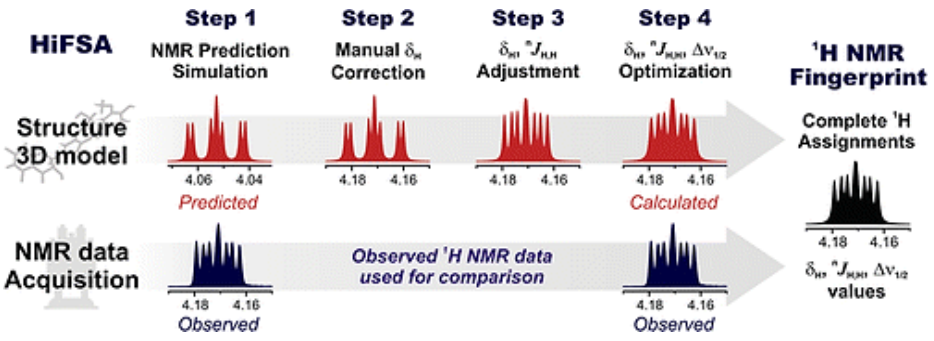

Scheme 1. Generation of the NMR Fingerprints by ^{1}H Iterative Full Spin Analysis (HiFSA), Exemplified with the Characteristic Resonance of H-8″ in Isomers 1–4

The HiFSA approach was exploited to investigate ^{1}H resonances that cannot be fully interpreted by simple visual inspection due to spectral overlap, as is the case of H-2″, H-6′, and even H-9″$_b$, which is partially obscured by the intense water peak in DMSO-d_6 (Figure 4). All ^{1}H,^{1}H scalar coupling constants were assessed, including several small, long-range couplings that influence the overall line shape of the aromatic ^{1}H NMR signals, such as the *p*-coupling between H-2′ and H-5′, $^5J_{H,H} \leq 0.6$ Hz. Moreover, HiFSA provided highly accurate ^{1}H chemical shift values for all ^{1}H resonances. This information was crucial to establishing spectral differences between the four flavonolignans, especially considering their near-identical *J*-coupling patterns. Overall, HiFSA led to the determination of twenty ^{1}H chemical shifts and fifteen scalar coupling constants for each isomer (Table 1). Although the high viscosity of DMSO-d_6 might cause sufficient line broadening to mask some small ($|^{4-6}J_{H,H}| < 0.5$ Hz) long-range coupling constants, the contribution of these small *J*-couplings to the overall line shape is included in the effective line width ($\Delta\nu_{1/2}$) of each NMR signal (see the Supporting Information).

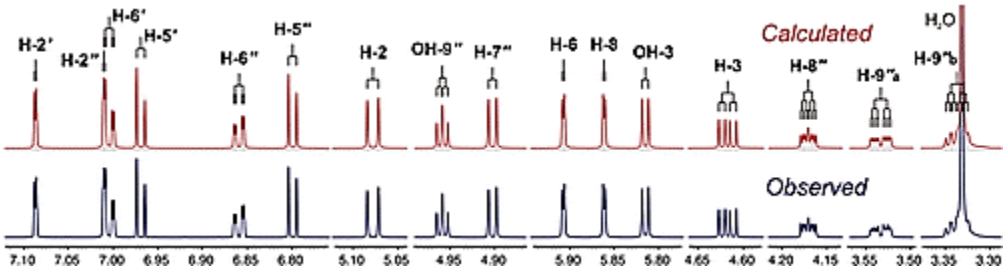

Figure 4. The ^{1}H NMR fingerprint of silybin A (**1**) generated by HiFSA (calculated, red) represents a detailed replica of the experimental 1D ^{1}H NMR spectrum (observed, blue, obtained in DMSO-d_6 at 900 MHz and 298 K). Complete ^{1}H assignments and simplified *J*-coupling trees are included, showing that the ^{1}H NMR spectrum of **1** can be largely interpreted under first order assumptions.

Table 1. ^{1}H Chemical Shifts (δ_H, in ppm) and ^{1}H,^{1}H Spin–spin Coupling Constants ($^nJ_{H,H}$, in Hz) of 1–4[a,b]

	δ_H (ppm)			
position	**1**	**2**	**3**	**4**
H-2	5.078	5.072	5.105	5.104
H-3	4.618	4.601	4.596	4.604
OH-3	5.815	5.810	5.836	5.833

OH-5	11.893	11.899	11.900	11.903
H-6	5.907	5.901	5.919	5.915
OH-7	10.848	10.850	10.857	10.866
H-8	5.861	5.860	5.884	5.879
H-2′	7.087	7.077	7.092	7.100
H-5′	6.970	6.973	6.933	6.932
H-6′	7.004	7.010	6.986	6.980
H-2″	7.010	7.013	7.003	7.004
OH-4″	9.158	9.159	9.159	9.158
H-5″	6.799	6.798	6.803	6.802
H-6″	6.859	6.861	6.854	6.854
H-7″	4.902	4.904	4.912	4.914
H-8″	4.171	4.161	4.160	4.167
H-9″$_a$	3.533	3.533	3.532	3.537
H-9″$_b$	3.337	3.339	3.339	3.335
OH-9″	4.959	4.962	4.957	4.953
OCH_3	3.773	3.776	3.776	3.775

	$^{n}J_{H,H}$ (Hz)			
coupling	**1**	**2**	**3**	**4**
^{3}J (H-2, H-3)	11.37	11.34	11.24	11.25
^{3}J (H-3, OH-3)	6.24	6.09	6.33	6.28
^{4}J (H-6, H-8)	2.11	2.13	2.09	2.11
^{5}J (H-2′, H-5′)	0.46	0.49	0.53	0.59
^{4}J (H-2′, H-6′)	2.05	2.07	2.06	2.07

^{3}J (H-5′, H-6′)	8.27	8.29	8.20	8.20
^{5}J (H-2″, H-5″)	0.59	0.51	0.54	0.57
^{4}J (H-2″, H-6″)	1.96	1.98	1.99	1.98
^{3}J (H-5″, H-6″)	8.06	8.05	8.01	8.01
^{3}J (H-7″, H-8″)	7.95	7.96	7.87	7.86
^{3}J (H-8″, H-9″$_a$)	2.50	2.51	2.61	2.63
^{3}J (H-8″, H-9″$_b$)	4.56	4.56	4.64	4.36
^{2}J (H-9″$_a$, H-9″$_b$)	–12.21	–12.23	–12.34	–12.35
^{3}J (H-9″$_a$, OH-9″)	5.15	5.07	5.13	5.15
^{3}J (H-9″$_b$, OH-9″)	5.86	5.90	5.83	5.94

a The δ_H and $^{n}J_{H,H}$ values were generated via ^{1}H iterative Full Spin Analysis (HiFSA) using experimental 1D ^{1}H NMR data acquired in DMSO-d_6 at 900 MHz and 298 K.

b The NMR samples were prepared at the following concentrations (in mg/mL): **1**, 1.48;**2**, 2.30; **3**, 1.91; **4**, 1.97.

Comparison of NMR Fingerprints

The HiFSA-generated ^{1}H NMR fingerprints, in combination with the complete ^{13}C assignments obtained from the DEPTQ, HSQC, and HMBC experiments (Table 2), provided a solid foundation for establishing chemical shift differences (Δδ) between compounds **1**–**4** (Figure 5). Considering the high digital resolution of ultrahigh-field NMR spectra (0.000029 ppm/pt at 900 MHz for ^{1}H and 0.00075 ppm/pt at 225 MHz for ^{13}C), Δδ values were expressed in parts per billion (ppb). In general, the chemical shift differences between the four flavonolignans were very small, with $\Delta\delta_H$ values of less than 40 ppb, and $\Delta\delta_C$ values below 500 ppb. In the case of the spectra of the diastereomers silybin A (**1**) and silybin B (**2**), the greatest $\Delta\delta_H$ was observed for H-3, with a downfield shift of only 17 ppb in **1** relative to **2**. Further notable changes affected H-2′ and H-8″, which are shifted 10 ppb downfield in **1**. As these three signals are located in clear regions of the ^{1}H NMR spectra, they are the most suitable for rapid discrimination of silybin diastereomers. In the ^{13}C domain, C-6′ showed the greatest $\Delta\delta_C$ with a 199 ppb downfield shift in **1** relative to **2**. In addition, C-2′ resonates 117 ppb upfield in **1**. Because these chemical shift changes point in opposite directions, the net difference (either in ppm or Hz) between the $\delta_C$values of C-6′ and C-2′ could be used to differentiate **1** and **2** as well.

Table 2. ^{13}C Chemical Shifts (δ_C, in ppm) of 1–4[a,b]

		δ_C (ppm)			
position	**type**	**1**	**2**	**3**	**4**
C-2	CH	82.539	82.496	82.524	82.463
C-3	CH	71.355	71.429	71.488	71.444
C-4	C	197.809	197.695	197.737	197.726
C-4a	C	100.430	100.373	100.473	100.452
C-5	C	163.274	163.287	163.301	163.301
C-6	CH	96.044	96.086	96.051	96.059
C-7	C	166.805	166.827	166.831	166.874
C-8	CH	95.019	95.066	95.048	95.051
C-8a	C	162.470	162.446	162.462	162.450
C-1′	C	130.041	130.105	130.303	130.302
C-2′	CH	116.531	116.648	116.462	116.433[c]
C-3′	C	143.245	143.222	142.879	142.914
C-4′	C	143.643	143.609	143.881	143.865
C-5′	CH	116.277	116.335	116.433	116.433[c]
C-6′	CH	121.373	121.174	120.893	120.934
C-1″	C	127.443	127.456	127.441	127.453
C-2″	CH	111.627	111.572	111.669	111.661
C-3″	C	147.592	147.608	147.568	147.567
C-4″	C	146.981	146.973	146.970	146.964
C-5″	CH	115.277	115.263	115.308	115.303
C-6″	CH	120.508	120.495	120.436	120.432
C-7″	CH	75.843	75.854	75.841	75.813

C-8″	CH	78.081	78.113	77.989	77.980
C-9″	CH_2	60.155	60.152	60.156	60.166
OCH_3	CH_3	55.655	55.653	55.665	55.662

a The δ_C values were obtained via the analysis of DEPTQ, HSQC, and HMBC experiments acquired in DMSO-d_6 at 298 K. DEPTQ experiments were recorded at 225 MHz. HSQC and HMBC experiments were collected at 600 MHz.

b The NMR samples were prepared at the following concentrations (in mg/mL): **1**, 1.48;**2**, 2.30; **3**, 1.91; **4**, 1.97.

c In isosilybin B (**4**), C-2′ and C-5′ are isochronous (see Figure 2).

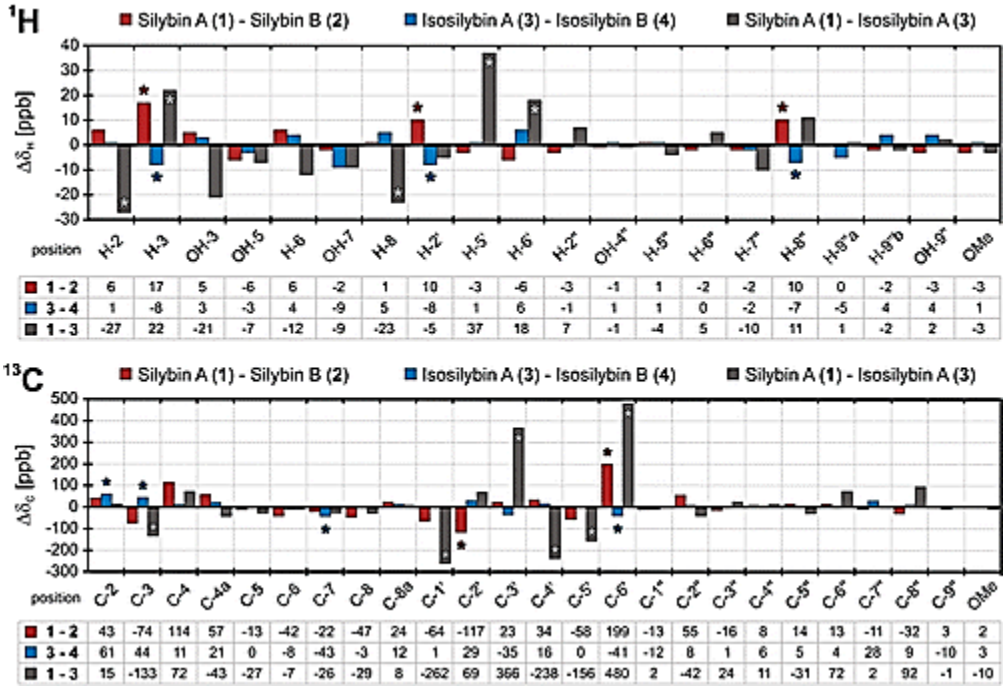

Figure 5. Graphical representation of the small chemical shift differences (Δδ, in ppb) between isomers **1**–**4** (DMSO-d_6, 298 K, 900 MHz for ^{1}H, 225 MHz for^{13}C). * denote diagnostic Δδ values to differentiate between diastereomeric pairs and regioisomers.

For the diastereomeric pair of isosilybin A (**3**) and isosilybin B (**4**), substantially smaller differences were observed in both ^{1}H and ^{13}C NMR spectra. Other than a $\Delta\delta_H$ of 9 ppb for the exchangeable proton OH-7, the greatest chemical shift differences were observed for H-3, H-2′ and H-8″, the same diagnostic nuclei that enabled discrimination of compounds **1** and **2**. However, the $\Delta\delta_H$ values between **3** and **4** did not exceed 8 ppb (0.008 ppm), with all upfield resonances belonging to **3**. Although these differences may appear negligible, 8 ppb is equivalent to 2.4 Hz at 300 MHz ^{1}H frequency. Therefore, these small differences in resonance frequency

are of the same order of magnitude as many small scalar coupling constants, such as *m*-couplings in benzene rings ($^4J_{H,H}$ ~ 2 Hz), which are readily measured in conventional 1D ^{1}H NMR spectra as digital resolution (typically 0.1 Hz/pt or better) is unlikely to be an issue. In the ^{13}C domain, C-2 exhibited the greatest $\Delta\delta_C$ of 61 ppb (13.7 Hz at 225 MHz ^{13}C frequency), however carbons C-3, C-7, and C-6′ were also identified as diagnostic resonances with $\Delta\delta_C$ values that were slightly over 40 ppb.

In addition to the distinction of diastereomeric pairs, the Δδ assessment also provided recognizable differences between the NMR profiles of regioisomeric silybins and isosilybins. A maximum $\Delta\delta_H$ value of 37 ppb was observed for H-5′, with the ^{1}H resonance in **1** located downfield relative to **3**. The signals of H-2, H-3, and H-8 displayed $\Delta\delta_H$ values in the 20–30 ppb range and, therefore, were identified as diagnostic resonances. Proportional to the intrinsically increased δ dispersion, somewhat greater Δδ differences were observed in the ^{13}C NMR spectra and primarily affected the B-ring. For example, C-6′ and C-3′ resonate 480 and 366 ppb downfield in **1** relative to **3**, respectively. In addition, carbons C-3, C-1′, C-4′, and C-5′ are shifted upfield in **1**, with $\Delta\delta_C$ values of 133, 262, 238, and 156 ppb, respectively.

Analysis of Complex Mixtures

After demonstrating the specificity of the HiFSA ^{1}H NMR fingerprints, the next step was to show that HiFSA-based methodology is independent of instrument and magnetic field, and capable of analyzing complex isomeric mixtures. The USP-certified silybin reference standard (SilybinUSP), representing a mixture of a subset of these regioisomers and diastereomers, was chosen as test material to evaluate the feasibility of the simultaneous identification and quantitation of **1**–**4**. Moreover, in order to explore this approach for different spectrometers and magnetic field strengths, ^{1}H NMR spectra were recorded at both 400 and 600 MHz. The experimental ^{1}H NMR spectra of Silybin USP were imported into PERCH, in conjunction with the ^{1}H NMR fingerprints of **1**–**4**. A simulated ^{1}H NMR spectrum of an equimolar mixture of the four flavonolignans was created by the PERCH spectral parameter editor. Next, the QMTLS iterators systematically honed the calculated parameters, adjusting all chemical shifts and integration areas until they matched the signal patterns observed in the experimental ^{1}H NMR spectrum (Figure 6). The result confirmed that Silybin USP contained a 1:1 mixture of **1** and **2**, i.e., silibinin.(24) The exact mole-to-mole ratio (r_i) of the two diastereomers was 0.498 of **1** to 0.502 of **2**. These values were consistent across the two instruments, thereby providing evidence for the reliability of both the quantitative conditions and the fitting approach. The overall composition (% w/w) of Silybin USP was determined by qHNMR as containing 47.8% of **1**, 48.2% of **2**, 2.9% of acetonitrile, and 1.0% of other flavonolignans. Small amounts (<0.1% w/w) of acetic acid and fatty/aliphatic material (calculated as stearic acid) were also present (see the Supporting Information). The isosilybins, **3** and **4**, were not detected.

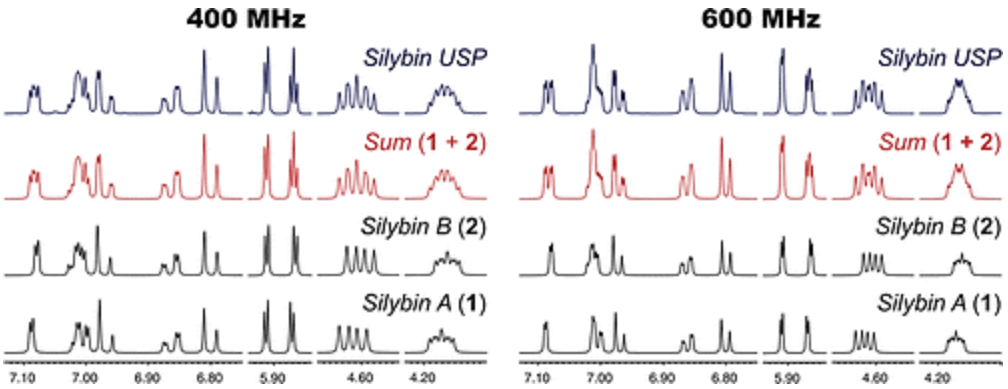

Figure 6. Simultaneous qualitative and quantitative ^{1}H NMR analysis of silybin USP reference standard performed at both 400 and 600 MHz (DMSO-d_6, 298 K). The intensity-adjusted fingerprints of silybin A (**1**) and silybin B (**2**) were generated by total line shape (TLS) iteration of the corresponding ^{1}H NMR profiles (see Table 1). The arithmetic addition of the two fingerprints (sum, red) matches the experimental 1D ^{1}H NMR spectrum (silybin USP, blue).

In a final step, the HiFSA-based methodology was applied to the parallel identification of **1**–**4** in a flavonolignan-enriched *Silybum* fraction, obtained by high-speed counter-current chromatography (HSCCC) analysis of silymarin, following the protocol established by Liu et al.[(79)] The total-line-shape fitting of the four ^{1}H NMR fingerprints enabled the assessment of individual contributions to the total area of the observed ^{1}H NMR spectrum, as well as the thorough interpretation of the complex resonance patterns (Figure 7). Consequently, the molar ratios of the four flavonolignans were readily assessed, showing that the fraction was enriched in **3** (r_3 = 0.484). The molar ratios of compounds **1**, **2**, and **4** were determined as 0.064, 0.231, and 0.221, respectively. It is noteworthy that the ^{1}H chemical shifts of the analytes in DMSO-$d_6$were reproducible, as only about 9% of the *final* δ_H measurements in the mixture showed deviations of more than 10 ppb when compared to the *initial* δ_H parameters of the HiFSA fingerprints. That is, these minor shifts affected only 6 out of 68 resonances used for quantitation, as the three downfield, exchangeable hydroxyl protons were not considered for this purpose. Furthermore, the greatest deviation from the initial δ_H values did not exceed 15 ppb (i.e., 4.5 Hz at 300 MHz ^{1}H frequency). Overall, the qualitative distinctions and quantitative measurements demonstrate that the regioisomers and diastereomers, **1**–**4**, can be identified unambiguously by NMR, despite the minute differences in their ^{1}H NMR profiles. Moreover, the HiFSA fingerprints not only allow mimicking complex signal patterns for the identification of individual components in the mixture, but also enable the simultaneous quantitation of the four isomers, even if their characteristic resonances cannot be individually integrated due to extensive spectral overlap (Figure 7).

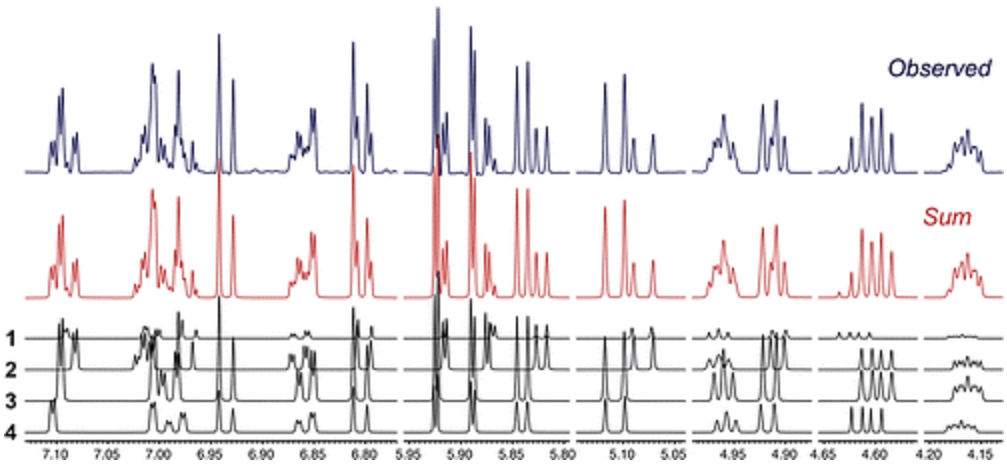

Figure 7. Simultaneous identification of silybin A (**1**), silybin B (**2**), isosilybin A (**3**), and isosilybin B (**4**) in a flavonolignan-enriched fraction obtained by HSCCC. The arithmetic addition of the four intensity adjusted fingerprints (sum, red) is in excellent agreement with the experimental ^{1}H NMR spectrum of the fraction (observed, blue, obtained in DMSO-d_6 at 600 MHz and 298 K).

Conclusions

This study illustrates the exceptional resolving power of contemporary NMR instrumentation, enabling the discrimination of four regioisomers and diastereomers which exhibit near-identical^{1}H NMR spectra. The very subtle spectroscopic differences of these isomers reflect their near-identical electronic environments, which result in very limited chemical shift dispersion combined with near-identical *J*-coupling patterns. The use of computer-assisted, ^{1}H iterative Full Spin Analysis (HiFSA) facilitated the interpretation of ^{1}H NMR data of pure isomers, the generation of their ^{1}H fingerprints, and the subsequent examination of mixtures of varying complexity. Although this study exploited the high sensitivity and spectral dispersion of ultrahigh-field NMR (900 MHz ^{1}H frequency) to establish small chemical shift differences, it also showed that silybin A (**1**), silybin B (**2**), isosilybin A (**3**), and isosilybin B (**4**) can be distinguished at ^{1}H frequencies as low as 400 MHz. Taking into account that most $\Delta\delta_H$ values fall in the low ppb range, the identification and quantitation of individual flavonolignans may be feasible even at 300 MHz. The magnitude of these chemical shift differences emphasizes the need for a third decimal place in the routine description and reporting of NMR data.

The capabilities of the HiFSA-based approach also address a long-standing bioanalytical challenge. *Silybum* preparations have attracted broad scientific interest due to their well-documented hepatoprotective properties, including treatment of chronic hepatitis C virus infection and advanced liver disease,[80] as well as cancer chemoprevention.[36, 37] However, considering the isomeric complexity of the milk thistle constituents and their significant differences in 3D structure, there is a need for more universal analytical methods with increased specificity for the individual isomers. The present results indicate that NMR can be superior to

chromatographic methods for the simultaneous identification and quantitation of the isomeric flavonolignans **1**–**4** in complex mixtures. High-quality reference materials of the*Silybum* flavonolignans are difficult to obtain but indispensable as standards for chromatographic analysis. The separation scheme developed by Graf et al.[68] enabled the production of high-purity samples of compounds **1**–**4**, as well as other *Silybum* constituents. The analysis of these samples by ECD and X-ray crystallography was essential to confirm the absolute configuration and, therefore, ensure the identity of each isomer.[29, 69] In addition to the universal nature of the HiFSA approach, the use of authenticated samples to generate high resolution ^{1}H NMR fingerprints eliminates the requirement for *identical* reference materials in future qHNMR studies.

The isolation and structure characterization of silybins and isosilybins is the result of an enormous research endeavor by many scientists over the past 60 years. Some seminal studies were carried out even before the spectroscopic techniques that could reveal the vast complexity of *Silybum* flavonolignans were available, and all these contributions are acknowledged. The newly demonstrated ability of computer-aided ^{1}H NMR analysis to unambiguously identify and quantify closely related regio- and diastereo-isomers such as compounds **1**–**4** represents a major step forward in *Silybum* research, and we anticipate that the studies described here will assist in shedding new light on the pharmacological properties of its constituents, as well as on the investigation of structure-activity relationships.

As part of an interesting study attempting to determine if two molecules can have NMR spectra so similar as to be indistinguishable from one another, Saielli and Bagno concluded that “it is difficult to generalize on the statement that two molecules cannot have the same NMR spectrum at all. Nevertheless, it seems unlikely that such an occurrence takes place, except perhaps when dealing with extremely simple or extremely crowded spectra (where information from NMR would be scarce or difficult to extract anyway)”.[81] The silybin/isosilybin case demonstrates that extreme situations where two or more molecules exhibit near-identical NMR profiles can occur, and actually are highly significant. The methodology described here represents a powerful and efficient way to distinguish such molecules, even if their chemical shift differences fall in the low ppb range. At the same time, HiFSA is able to extract key NMR parameters from crowded spectral regions, thereby detecting differences that might otherwise remain unknown. Because HiFSA enables a better understanding of complex NMR signals and provides accurate δ values for all resonances, this approach has the potential to advance the study of complex and potentially hidden configurational problems in organic chemistry.

Experimental Section

Materials

The certified silybin reference standard was kindly provided by the United States Pharmacopeial Convention Inc. (Rockville, MD). The silymarin sample subjected to HSCCC fractionation was

purchased from Sigma-Aldrich Inc. (St. Louis, MO). Hexadeuterodimethyl sulfoxide (DMSO-d_6, D 99.9%) was obtained from Cambridge Isotope Laboratories, Inc. (Andover, MA). Standard 5 mm, 7 in. NMR tubes (XR-55 series) from Norell Inc. (Landisville, NJ) were used for all NMR analyses.

Isolation and Preliminary Analysis of Silybins and Isosilybins

High-purity, authenticated samples of silybin A (**1**), silybin B (**2**), isosilybin A (**3**), and isosilybin B (**4**) were obtained as described in detail previously.[68] The samples were >99% w/w pure as evaluated under two different conditions by UPLC (see the Supporting Information) on an ACQUITY system with data collected and analyzed using Empower 2 software (Waters Corp., Milford, MA). Condition 1 consisted of a gradient that began with a mixture of MeOH and H_2O in a volume ratio of 30:70 and increased linearly to 60:40 over 10 min, using an HSS-T3 column (1.8 μm, 2.1 × 100 mm) and a flow rate of 0.40 mL/min. Condition 2 was isocratic using a mixture of MeCN and H_2O in a volume ratio of 20:80 (0.1% formic acid) for 10 min for compounds **1** and **2**, or 15 min for **3** and **4**, using a BEH-Phenyl column (1.7 μm, 2.1 × 100 mm) and a flow rate of 0.50 mL/min. For both conditions, the columns were heated to 40 °C. A PDA detector was used to monitor the absorbance of the eluent at 210, 288, and 450 nm. Preliminary NMR evaluation of**1**–**4** in DMSO-d_6 was carried out on a JEOL ECA-500 spectrometer operating at 500.15 MHz ^{1}H frequency.

HSCCC Analysis of Silymarin

The HSCCC separation was conducted on a TBE-300A instrument (Shanghai Tauto Biotech Co. Ltd., Shanghai, China) with three multilayer coil separation columns connected in series (tubing inner diameter = 1.6 mm; total column volume = 280 mL). The revolution radius (distance between the holder axis and the central axis of the centrifuge, R) was 5 cm, and the β values of the multilayer coil varied from 0.5 at the internal terminal to 0.8 at the external terminal ($\beta = r/R$; where r is the distance from the edge of the coil to the holder shaft). The rotational speed of the apparatus was regulated with a speed controller with the range 0–1000 rpm. A constant temperature-circulating bath was used to control the temperature at 298 K (25 °C). The HSCCC system was equipped with a single-piston solvent pump, a fixed wavelength UV–vis detector with a preparative flow cell, and a fraction collector. Data were recorded on a chromatography data handling system and then transferred to a spreadsheet for further analysis.

The solvent system was prepared by mixing hexane, $CHCl_3$, MeOH, and 0.5% v/v aqueous acetic acid in a volume ratio of 1:22:20:12, respectively. The resulting mixture was equilibrated in a separatory funnel at room temperature, and the two phases were separated. The upper phase was aqueous. Samples were prepared by suspending 0.2 g of silymarin in 5 mL of upper phase and 5 mL of lower phase. The biphasic mixture was then filtered and loaded into a 20 mL sample loop. The remaining 10 mL volume was filled with lower phase. The HSCCC tubing was then filled with the upper stationary phase with no rotation. Next, the coils were rotated at 1000 rpm

as the lower mobile phase was pumped at a flow rate of 2 mL/min from head-to-tail. To begin the run, the silymarin sample was injected onto the column. The UV–vis detector monitored the absorption of the eluent at 254 nm, and fractions were collected at 10 mL/tube. After 450 mL of mobile phase had eluted from the column (partition coefficient, K = 1.8), aqueous phase was pumped into the column while the centrifuge was left running (elution-extrusion CCC). The run was stopped after 300 mL of aqueous phase had been introduced into the column. The stationary phase retention factor was determined to be 79% based on the measured void volume.
The K value of isosilybins A and B (**3**, **4**) was 0.64, while the K value of silybins A and B (**1**, **2**) was 0.76 in this solvent system.

The collected fractions were reduced in volume and analyzed by thin layer chromatography (TLC) using precoated, 0.20-mm thick, silica gel G/UV_{254} plates (20 × 10 cm). The TLC plates were developed at room temperature using a mixture of $CHCl_3$, MeOH, and H_2O in a volume ratio of 150:20:1, respectively. Plates were dipped in a general-purpose reagent (*p*-anisaldehyde/sulfuric acid/acetic acid, 1:1:48), drained, and heated at 95 °C for 5 min. TLC chromatograms were scanned for digital preservation at 150 dpi. On the basis of their TLC profiles, 20 of the collected fractions were selected for NMR analysis. Because of the complexity of the signal patterns in its ^{1}H NMR spectrum, fraction 21 was selected for further investigation by HiFSA.

NMR Sample Preparation

NMR samples of **1**–**4** were prepared by precisely weighing 1–2 mg (±0.01 mg) directly into the NMR tubes using a high precision analytical balance, followed by the addition of 600 μL of DMSO-d_6 using a Pressure-Lok gas syringe (VICI Precision Sampling, Inc., Baton Rouge, LA). NMR samples of the silybin USP reference standard and the flavonolignan-enriched HSCCC fraction were prepared by precisely weighing 5–10 mg (±0.01 mg) and following the procedure described above.

NMR Spectroscopy

NMR measurements were recorded at 400.17, 600.13, and 899.94 MHz. The 400 MHz spectrometer was equipped with a 5-mm, direct detection, broadband observe (BBO) room temperature probe. The 600 and 900 MHz spectrometers were equipped with 5-mm, triple resonance inverse detection TXI and TCI cryoprobes, respectively. All NMR experiments were acquired under temperature-controlled conditions at 298 K (25 °C), and the probes were frequency tuned and impedance matched prior to each data collection. Chemical shifts (δ) are expressed in ppm with reference to the residual solvent signals (2.500 ppm for ^{1}H, 39.510 ppm for ^{13}C) and internal TMS (0.000 ppm). Scalar coupling constants (J) are given in Hertz.

Quantitative 1D ^{1}H NMR (qHNMR) spectra were recorded using a 90° single-pulse experiment. The 90° pulse was calibrated by evaluating the null at 360° and back-calculating the corresponding pulse width as $pw_{90} = 1/4 \times pw_{360}$. The following acquisition parameters were

used: a spectral width of 30 ppm (centered at 7.5 ppm), an acquisition time of 4.0 s, and a relaxation delay of 60 s ($\geq 5 \times T_1$). The 1D ^{1}H NMR data were processed with NUTS software (v.201004, Acorn NMR, Inc., Las Positas, CA) using Lorentzian-to-Gaussian apodization for resolution enhancement (line broadening = −1.0 Hz, Gaussian factor = 0.10), followed by zero filling to 256K data points prior to Fourier transformation. The resulting NMR spectra were subjected to manual phase adjustment and baseline correction using fifth-order polynomial functions. DEPTQ spectra were recorded at 225.31 MHz using a spectral width of 220 ppm, an acquisition time of 1.0 s, and a relaxation delay of 1.0 s. DEPTQ data processing was carried out in Mnova software (v.8.0.0–10524, Mestrelab Research S.L., Santiago de Compostela, Spain) using Lorentzian-to-Gaussian apodization (line broadening = −3.0 Hz, Gaussian factor = 0.30), zero-filling to 256K data points, manual phasing, and a third-order polynomial baseline correction.

All 2D experiments were recorded at 600.13 MHz with 2K data points in F_2 and 256 increments in F_1. The ^{1}H,^{1}H-COSY experiments were acquired in magnitude mode using a spectral width of 12 ppm in each dimension, an acquisition time of 0.29 s in F_2, and a relaxation delay of 1.0 s. The ^{1}H,^{13}C-HSQC and HMBC experiments were acquired in phase-sensitive mode (States-TPPI or Echo-Antiecho for quadrature detection in F_1) with a spectral width of 12 ppm and an acquisition time of 0.29 s in F_2, plus a relaxation delay of 1.5 s. HSQC and HMBC experiments were recorded with spectral widths in the F_1-dimension of 170 and 220 ppm, respectively. Semiselective ^{1}H,^{13}C-HMBC experiments were acquired in magnitude mode with a spectral width of 20 ppm in F_1 (centered at 145 ppm), an acquisition time of 0.25 s in F_2, and a relaxation delay of 0.5 s. All HMBC-type experiments were recorded with an optimized delay of 0.25 s for evolution of long-range heteronuclear couplings (i.e., $^{2,3}J_{C,H}$ = 4 Hz). Subsequent 2D NMR data processing was carried out with Mnova software. The 2D data sets were zero filled to 4K data points in F_2, linear predicted to 2K, and zero-filled to 4K data points in F_1 in order to obtain 4K × 4K spectral data matrices. After Fourier transformation, 2D NMR experiments were phase-adjusted, if necessary, and baseline-corrected using third-order polynomial functions.

Computational Analysis

The ^{1}H iterative Full Spin Analysis (HiFSA) was performed with PERCH NMR software (v.2011.1, PERCH Solutions Ltd., Kuopio, Finland). The resolution-enhanced 1D ^{1}H NMR spectra were imported into the PERCH shell as JCAMP-DX files using the IMP module. Further postprocessing operations were carried out with the PAC program. The 3D molecular structure assembly, geometry optimization, conformational analysis, and NMR prediction were performed using PERCH's Molecular Modeling Software (MMS). Direct comparisons between the simulated and observed NMR spectra, as well as manual chemical shift correction, were carried out in the spectral parameters (PMS) module. The optimization of calculated NMR parameters was achieved with the program PERCHit in three steps: (i) analysis of discrete spin systems using the integral-transform mode; (ii) evaluation of the complete ^{1}H NMR spectrum using the total-line-fitting mode; and (iii) optimization of Gaussian and dispersion contributions to line

shape, also using the total-line-fitting mode. Iterative optimization was performed until an excellent agreement between the observed and simulated spectra was reached, that is, convergence with a total intensity rmsd below 0.1%. The optimized NMR parameters of **1**–**4** were stored in individual PERCH parameters (.pms) text files (see the Supporting Information).

For the examination of mixtures, the resolution-enhanced ^{1}H NMR spectrum of the sample was imported into the PERCH shell as described above. The ^{1}H NMR profiles of **1**–**4** were combined into a single .pms text file (see the Supporting Information) and imported into the PMS module. The four ^{1}H fingerprints were simultaneously fitted to the experimental NMR spectra of the mixture using PERCHit and the three-step optimization protocol. To avoid distortion of known signal splitting patterns, the optimized *J* values were kept constant ("fixed") during the iteration. The relative molar abundances of **1**–**4** (as mol %) were automatically calculated by PERCHit as part of the population optimization process.

Supporting Information

Numbering systems, UPLC chromatograms, 1D/2D NMR experiments, qHNMR composition profiles, and PERCH-generated ^{1}H NMR fingerprints of **1**–**4**. This material is available free of charge via the Internet at http://pubs.acs.org.

The authors declare no competing financial interest.

Acknowledgment

We thank M. Niemitz and Dr. S.-P. Korhonen (PERCH Solutions Ltd., Kuopio, Finland) for their valuable comments on ^{1}H Full Spin Analysis and TLS fitting as well as many helpful suggestions in the context of computational NMR analysis. Dr. B. Ramirez is acknowledged for his valued support in the NMR facility at the UIC Center for Structural Biology (CSB). The research at the University of Illinois at Chicago was funded by the National Institutes of Health (NIH)/National Center for Complementary and Alternative Medicine (NCCAM) through Grant No. RC2 AT005899. Samples of silybin A, silybin B, isosilybin A, and isosilybin B were isolated and characterized at the University of North Carolina at Greensboro with support from NIH/NCCAM via Grant No. R01 AT006842 and the NIH/National Institute of General Medical Sciences (NIGMS) via Grant No. R01 GM077482. During the preparation of this manuscript, J.G.N. was supported in part by the United States Pharmacopeial Convention as part of the 2012/2013 USP Global Research Fellowship Program. The construction of the UIC CSB and the 900 MHz (21.1 T) NMR spectrometer was funded by NIGMS Grant No. P41 GM068944.

References

1. Günther, H. *NMR Spectroscopy: Basic Principles, Concepts, And Applications in Chemistry*,2nd ed.; Wiley: Chichester, **1995**; Chapter 6, pp 199– 219.

2. Wiley, R. H.; Crawford, T. H.; Staples, C. E. *J. Org. Chem.* **1962**, 27, 1535– 1539

3. Abraham, R. J.; Warne, M. A.; Griffiths, L. *Magn. Reson. Chem.* **1998**, 36, S179–S188

4. Abraham, R. J.; Canton, M.; Griffiths, L. *Magn. Reson. Chem.* **2001**, 39, 421–431

5. Abraham, R. J.; Reid, M. *Magn. Reson. Chem.* **2000**, 38, 570– 579

6. Bifulco, G.; Dambruoso, P.; Gomez-Paloma, L.; Riccio, R. *Chem. Rev.* **2007**, 107, 3744–3779

7. Hänsel, R.; Schopflin, G. *Tetrahedron Lett.* **1967**, 8, 3645– 3648

8. Hänsel, R.; Schulz, J.; Pelter, A. *J. Chem. Soc., Chem. Commun.* **1972**, 195– 196

9. Hänsel, R.; Schulz, J.; Pelter, A. *Chem. Ber.* **1975**, 108, 1482– 1501

10. Hänsel, R.; Schulz, J.; Pelter, A.; Rimpler, H.; Rizk, A.-F. M. *Tetrahedron Lett.* **1969**, 51,4417– 4420

11. Janiak, I. B.; Hänsel, R. *Planta Med.* **1960**, 8, 71– 84

12. Merlini, L.; Zanarotti, A.; Pelter, A.; Rochefort, M. P.; Hänsel, R. *J. Chem. Soc., Chem. Commun.* **1979**, 695

13. Pelter, A.; Hänsel, R. *Tetrahedron Lett.* **1968**, 9, 2911– 2916

14. Pelter, A.; Hänsel, R. *Chem. Ber.* **1975**, 108, 790– 802

15. Abraham, D. J.; Takagi, S.; Rosenstein, R. D.; Shiono, R.; Wagner, H.; Hoerhammer, L.; Seligmann, O.; Farnsworth, N. R. *Tetrahedron Lett.* **1970**, 2675– 2678

16. Lotter, H.; Wagner, H. *Z. Naturforsch., C: Biosci.* **1983**, 38C, 339– 341

17. Tittel, G.; Wagner, H. *J. Chromatogr.* **1977**, 135, 499– 501

18. Tittel, G.; Wagner, H. *J. Chromatogr.* **1978**, 153, 227– 232

19. Wagner, H.; Diesel, P.; Seitz, M. *Arzneim. Forsch.* **1974**, 24, 466– 471

20. Wagner, H.; Hoerhammer, L.; Muenster, R. *Arzneim. Forsch.* **1968**, 18, 688– 696

21. Wagner, H.; Hoerhammer, L.; Münster, R. *Naturwissenschaften* **1965**, 52, 305

22. Wagner, H.; Seligmann, O.; Hoerhammer, L.; Seitz, M.; Sonnenbichler, J. *Tetrahedron Lett.* **1971**, 12, 1895– 1899

23. Wagner, H.; Seligmann, O.; Seitz, E.; Abraham, D.; Sonnenbichler, J. *Z. Naturforsch. B***1976**, 31B, 876– 884

24. Kroll, D. J.; Shaw, H. S.; Oberlies, N. H. *Integr. Cancer Ther.* **2007**, 6, 110– 119

25. Mascher, H.; Kikuta, C.; Weyhenmeyer, R. *J. Liq. Chromatogr.* **1993**, 16, 2727– 2789

26. Rickling, B.; Hans, B.; Kramarczyk, R.; Krumbiegel, G.; Weyhenmeyer, R. *J. Chromatogr. B***1995**, 670, 267– 277

27. Kren, V.; Kubisch, J.; Sedmera, P.; Halada, P.; Prikrylova, V.; Jegorov, A.; Cvak, L.; Gebhardt, R.; Ulrichova, J.; Simanek, V. *J. Chem. Soc., Perkin Trans. 1* **1997**, 2467–2474

28. Kren, V.; Ulrichova, J.; Kosina, P.; Stevenson, D.; Sedmera, P.; Prikrylova, V.; Halada, P.; Simanek, V. *Drug Metab. Dispos.* **2000**, 28, 1513– 1517

29. Kim, N.-C.; Graf, T. N.; Sparacino, C. M.; Wani, M. C.; Wall, M. E. *Org. Biomol. Chem.***2003**, 1, 1684– 1689

30. Kim, N.-C.; Graf, T. N.; Sparacino, C. M.; Wani, M. C.; Wall, M. E. *Org. Biomol. Chem.***2003**, 1, 3470

31. Lee, D. Y. W.; Liu, Y. *J. Nat. Prod.* **2003**, 66, 1632

32. Lee, D. Y. W.; Liu, Y. *J. Nat. Prod.* **2003**, 66, 1171– 1174

33. Morazzoni, P.; Bombardelli, E. *Fitoterapia* **1995**, 66, 3– 42

34. Corchete, P. In *Bioactive Molecules and Medicinal Plants*; Ramawat, K. G.; Merillon, J. M., Eds.; Springer: Berlin, **2008**; Chapter 6, pp 123– 148.

35. Abenavoli, L.; Capasso, R.; Milic, N.; Capasso, F. *Phytother. Res.* **2010**, 24, 1423–1432

36. Agarwal, R.; Agarwal, C.; Ichikawa, H.; Singh, R. P.; Aggarwal, B. B. *Anticancer Res.* **2006**,26, 4457– 4498

37. Ramasamy, K.; Agarwal, R. *Canc. Lett.* **2008**, 269, 352– 362

38. Polyak, S. J.; Oberlies, N. H.; Pécheur, E.-I.; Ferenci, P.; Pawlotsky, J.-M. *Antivir. Ther.***2013**, in press, DOI: 10.3851/IMP2402.

39. Deep, G.; Oberlies, N. H.; Kroll, D. J.; Agarwal, R. *Int. J. Cancer* **2008**, 123, 41–50

40. Polyak, S. J.; Morishima, C.; Lohmann, V.; Pal, S.; Lee, D. Y. W.; Liu, Y.; Graf, T. N.; Oberlies, N. H. *Proc. Natl. Acad. Sci. U.S.A.* **2010**, 107, 5995– 5999

41. Brantley, S. J.; Oberlies, N. H.; Kroll, D. J.; Paine, M. F. *J. Pharmacol. Exp. Ther.* **2010**,332, 1081– 1087

42. Schrieber, S. J.; Hawke, R. L.; Wen, Z.; Smith, P. C.; Reddy, K. R.; Wahed, A. S.; Belle, S. H.; Afdhal, N. H.; Navarro, V. J.; Meyers, C. M.; Doo, E.; Fried, M. W. *Drug Metab. Dispos.***2011**, 39, 2182– 2190

43. Quaglia, M. G.; Bossu, E.; Donati, E.; Mazzanti, G.; Brandt, A. *J. Pharm. Biomed. Anal.***1999**, 19, 435– 442

44. Ding, T. M.; Tian, S. J.; Zhang, Z. X.; Gu, D. Z.; Chen, Y. F.; Shi, Y. H.; Sun, Z. P. *J. Pharm. Biomed. Anal.* **2001**, 26, 155– 161

45. Kvasnicka, F.; Biba, B.; Sevcik, R.; Voldrich, M.; Kratka, J. *J. Chromatogr. A* **2003**, 990,239– 245

46. Zhao, Y.; Chen, B.; Yao, S. *J. Pharm. Biomed. Anal.* **2005**, 38, 564– 570

47. Lee, J. I.; Narayan, M.; Barrett, J. S. *J. Chromatogr. B* **2007**, 845, 95– 103

48. Shibano, M.; Lin, A.-S.; Itokawa, H.; Lee, K.-H. *J. Nat. Prod.* **2007**, 70, 1424– 1428

49. Wang, K.; Zhang, H.; Shen, L.; Du, Q.; Li, J. *J. Pharm. Biomed. Anal.* **2010**, 53, 1053–1057

50. Kuki, A.; Nagy, L.; Deak, G.; Nagy, M.; Zsuga, M.; Keki, S. *Chromatographia* **2012**, 75, 175–180

51. Pauli, G. F.; Jaki, B. U.; Gödecke, T.; Lankin, D. C. *J. Nat. Prod.* **2012**, 75, 834– 851

52. Pauli, G. F.; Jaki, B. U.; Lankin, D. C. *J. Nat. Prod.* **2005**, 68, 133– 149

53. Malz, F.; Jancke, H. *J. Pharm. Biomed. Anal.* **2005**, 38, 813– 823

54. Kim, H. K.; Wilson, E. G.; Choi, Y. H.; Verpoorte, R. *Planta Med.* **2010**, 76, 1094–1102

55. Robinette, S. L.; Brüschweiler, R.; Schroeder, F. C.; Edison, A. S. *Acc. Chem. Res.* **2012**,45, 288– 297

56. Gottlieb, O. R. *Phytochemistry* **1972**, 11, 1537– 1570

57. Merlini, L.; Zanarotti, A. *Tetrahedron Lett.* **1975**, 3621– 3622

58. Dewick, P. M. *Medicinal Natural Products: a Biosynthetic Approach*, 3rd ed.; John Wiley & Sons: Chichester, **2009**; pp 173– 174.

59. Napolitano, J. G.; Lankin, D. C.; Chen, S.-N.; Pauli, G. F. *Magn. Reson. Chem.* **2012**, 50,569– 575

60. Napolitano, J. G.; Gödecke, T.; Rodriguez Brasco, M. F.; Jaki, B. U.; Chen, S.-N.; Lankin,D. C.; Pauli, G. F. *J. Nat. Prod.* **2012**, 75, 238– 248

61. Afifi, M. S. A.; Ahmed, M. M.; Pezzuto, J. M.; Kinghorn, A. D. *Phytochemistry* **1993**, 34,839– 841

62. Guz, N. R.; Stermitz, F. R. *J. Nat. Prod.* **2000**, 63, 1140– 1145

63. Higashibayashi, S.; Czechtizky, W.; Kobayashi, Y.; Kishi, Y. *J. Am. Chem. Soc.* **2003**, 125,14379– 14393

64. Curran, D. P.; Zhang, Q.; Lu, H.; Gudipati, V. *J. Am. Chem. Soc.* **2006**, 128, 9943–9956

65. Oishi, T.; Kanemoto, M.; Swasono, R.; Matsumori, N.; Murata, M. *Org. Lett.* **2008**, 10,5203– 5206

66. Miyauchi, H.; Ikematsu, C.; Shimazaki, T.; Kato, S.; Shinmyozu, T.; Shimo, T.; Somekawa,K. *Tetrahedron* **2008**, 64, 4108– 4116

67. Zhang, K.; Curran, D. P. *Synlett* **2010**, 667– 671

68. Graf, T. N.; Wani, M. C.; Agarwal, R.; Kroll, D. J.; Oberlies, N. H. *Planta Med.* **2007**, 73,1495– 1501

69. Sy-Cordero, A. A.; Day, C. S.; Oberlies, N. H. *J. Nat. Prod.* **2012**, 75, 1879– 1881

70. Malz, F. In *NMR Spectroscopy in Pharmaceutical Analysis*; Holzgrabe, U.; Wawer, I.; Diehl,B., Eds.; Elsevier Ltd.: Oxford, UK, **2008**; Chapter 2, pp 43– 62.

71. Pauli, G. F.; Jaki, B. U.; Lankin, D. C.; Walter, J. A.; Burton, I. W. In *Bioactive Natural Products: Detection, Isolation and Structural Determination*, 2nd ed.; Colegate, S. M.;Molyneux, R. J., Eds.; Taylor & Francis/CRC Press: New York, **2008**; Chapter 4, pp 113–142.

72. Pierens, G. K.; Carroll, A. R.; Davis, R. A.; Palframan, M. E.; Quinn, R. J. *J. Nat. Prod.***2008**, 71, 810– 813

73. Gödecke, T.; Yao, P.; Napolitano, J. G.; Nikolić, D.; Dietz, B. M.; Bolton, J. L.; van Breemen, R. B.; Farnsworth, N. R.; Chen, S.-N.; Lankin, D. C.; Pauli, G. F. *Fitoterapia***2012**, 83, 18– 32

74. Burger, R.; Bigler, P. *J. Magn. Reson.* **1998**, 135, 529– 534

75. Claridge, T. D. W.; Perez-Victoria, I. *Org. Biomol. Chem.* **2003**, 1, 3632– 3634

76. Laatikainen, R.; Niemitz, M.; Weber, U.; Sundelin, J.; Hassinen, T.; Vepsalainen, J. *J. Magn. Reson., Ser. A* **1996**, 120, 1– 10

77. Laatikainen, R.; Niemitz, M.; Malaisse, W. J.; Biesemans, M.; Willem, R. *Magn. Res. Med.***1996**, 36, 359– 365

78. Laatikainen, R.; Tiainen, M.; Korhonen, S.-P.; Niemitz, M. In *Encyclopedia of Magnetic Resonance*; Harris, R. K.; Wasylishen, R. E., Eds.; John Wiley & Sons, Ltd.: Chicester,**2011**.

79. Liu, H.; Yuan, Q.; Li, C. F.; Huang, T. X. *Process Biochem.* **2010**, 45, 799– 804

80. Seeff, L. B.; Curto, T. M.; Szabo, G.; Everson, G. T.; Bonkovsky, H. L.; Dienstag, J. L.; Shiffman, M. L.; Lindsay, K. L.; Lok, A. S. F.; DiBisceglie, A. M.; Lee, W. M.; Ghany, M. G.*Hepatology* **2008**, 47, 605– 612

81. Saielli, G.; Bagno, A. *Org. Lett.* **2009**, 11, 1409– 1412